Chalcogenide Letters Vol. 11, No. 9, September 2014, p. 461 - 470

EFFECTS OF DOPANT'S PROFILE ON PHYSICAL PROPERTIES OF ZnTe THIN FILMS

G.H. TARIQ[a,*], N.A. NIAZ[b], M. ANIS-UR-REHMAN[a]
[a]*Applied Thermal Physics Laboratory, Department of Physics, COMSATS Institute of Information Technology, Islamabad, Pakistan*
[b]*Department of Physics, Bahauddin Zakariya University Multan, Pakistan*

ZnTe thin films of 300nm thickness were prepared on glass substrates by thermal evaporation. These thin films were annealed in vacuum at 400°C for an hour, thereafter these films were immersed in $Cu(NO_3)_2.H_2O$ solution (1g/1000ml) for 20 minutes for Cu doping. Furthermore these doped samples were annealed in vacuum for diffusion of Cu in thin films for different annealing temperatures (one sample as doped, samples annealed after doping at 100°C - 400°C) for one hour with interval of 100°C. The crystalline nature and other structural parameters like lattice parameter, dislocation density and microstrain were analyzed by X-ray diffraction (XRD). The optical properties, such as transmission spectra, absorption coefficient, band gap and optical density were investigated with a UV–VIS-NIR spectrophotometer. The determined band gap was shifted from 2.22eV to 2.19eV with annealing. The resistivity of as doped sample was 148 Ω-cm and after annealing at 400°C it was reduced to 30 Ω-cm. The conductivity type was investigated by hot probe method and was found p-type.

(Received June 30, 2014; Accepted September 29, 2014)

Keywords: solar cells, crystalline, ZnTe, dopant

1. Introduction

Photovoltaic solar cells based on CdTe polycrystalline thin films are promising for low cost large scale manufacturing due to their low cost material, high absorption coefficient and stability [1, 2]. These solar cells can be manufactured with low film thickness (1-1.5μm) [3]. At present the module efficiency of CdTe thin film solar cells (TFSC) is in the range of 10% only, the opportunity of improving efficiency of these TFSC is high. One of the main issues of low efficiency of these TFSCs is non-ohmic back contact with the p-type CdTe because no metal is available with work function for ohmic contact with p-type CdTe [4]. This issue could be overcomed by incorporating an interfacial layer between p-type CdTe thin film and suitable metal back contact layer. Such interfacial layer should have small band offset with p-type CdTe thin film [5]. ZnTe has small band offset value of ~0.1eV [6] and is a good candidate for interfacial layer [7] in CdTe based TFSCs. An interfacial layer must facilitate high p-type doping to provide low resistance at back contact, ZnTe exhibited p-type doping with Cu [5]. Researchers have used a variety of doping techniques including diffusion, co-evaporation, ion exchange process etc. However, due to simplicity and low cost, ion exchange process is commonly utilized for doping of II-VI semiconductors including ZnTe by Ag, In and Cu [8, 9].

In the present work, we deposited ZnTe thin films by thermal evaporation method and Cu doping was achieved by ion exchange route. These doped thin films were annealed in vacuum at different temperatures. Further the effects of dopant and annealing temperatures on the structural and optical properties were studied.

*Corresponding author: g.hasnain@yahoo.com

2. Experimental

Thin films of ZnTe with thickness 0.3µm were prepared on glass substrates by thermal evaporation. ZnTe in powder form of purity 99.99% was used as precursor. Thin films were deposited in vacuum ~$2x10^{-5}$ mbar at the chamber ambient temperature of ~106°C. Before deposition, substrates were first cleaned by detergent and filtered water and then in ultrasonic bath cleaner using distilled water. Finally these substrates were cleaned ultrasonically in isopropyl alcohol (IPA) [10]. The ZnTe powder was placed in a molybdenum boat. The source to substrate distance during depositions was kept 15cm. Source current was applied after achieving a vacuum ~$2x10^{-5}$ mbar in the chamber. The source current was increased slowly to heat the source material. Controlling all parameters i.e. vacuum level, substrate temperature, evaporation rate, source current etc, source shutter was moved and allowed the ZnTe source material species to start depositing on the substrate. After depositing thin film of required thickness shutter was closed. The source current was turned off and chamber was cooled down to room temperature. All prepared samples were annealed in vacuum ~$3x10^{-4}$mbar for an hour at 400°C. Then these samples were immersed in $Cu(NO_3)_2.H_2O$ solution (1g/1000ml) for 20 minutes for Cu doping. After immersion, these samples were cleaned in distilled water and dried by hot compressed air. Further these doped samples were annealed in vacuum for different annealing temperatures (one sample as doped, annealed after doping at 100°C - 400°C) for one hour with interval of 100°C. Annealing before doping and after doping at different temperatures is given in table 1.

Table 1: Annealing of ZnTe thin films before and after doping

Sample	Annealing in vacuum ~$8x10^{-5}$mbar for 1 hour	
	Before doping	After doping
ZT-1	400°C	Not annealed
ZT-2	400°C	100°C
ZT-3	400°C	200°C
ZT-4	400°C	300°C
ZT-5	400°C	400°C

3. Characterization

Cu doped ZnTe thin films were characterized by studying mainly structural properties like the crystalline nature, lattice parameter, dislocation density and microstrain by using X-ray diffraction (XRD). Optical properties such as transmission spectra, absorption coefficient, bandgap and optical density were investigated with a UV–VIS-NIR spectrophotometer (Perkin Elmer Lamda 950). XRD characterizations were done by using PANalytical X'Pert PRO XRD with CuKα radiation (λ = 1.5406 Å). These XRD measurements were taken for 20° to 60° values of 2θ. The elemental composition of prepared thin films was obtained by using energy-dispersive X-ray (EDX) and data is given in the table 2. The conductivity type of Cu doped ZnTe films was investigated by hot probe method measuring the potential difference between a hot and cold contact [11, 12].

Table 2: Elemental composition (at.%) of doped ZnTe thin films

Sample	Zn at.%	Te at.%	Cu at.%
Not annealed	43.34	44.07	12.59
100°C	43.56	43.69	12.75
200°C	42.56	44.24	13.20
300°C	43.27	44.06	12.67
400°C	43.15	44.11	12.74

4. Results and discussion:

4.1 Structural Characterizations

Fig 1 shows the X-ray diffraction (XRD) patterns of one sample as doped (not annealed) and samples annealed after doping ZnTe thin films at different temperatures. These XRD measurements provide insight into the structural properties of these thin films. XRD patterns of films exhibit polycrystalline nature of these doped ZnTe thin films. All these films reveal cubic structure with preferential orientation along the (111) planes and this peak fits well with JCPDS reference data.

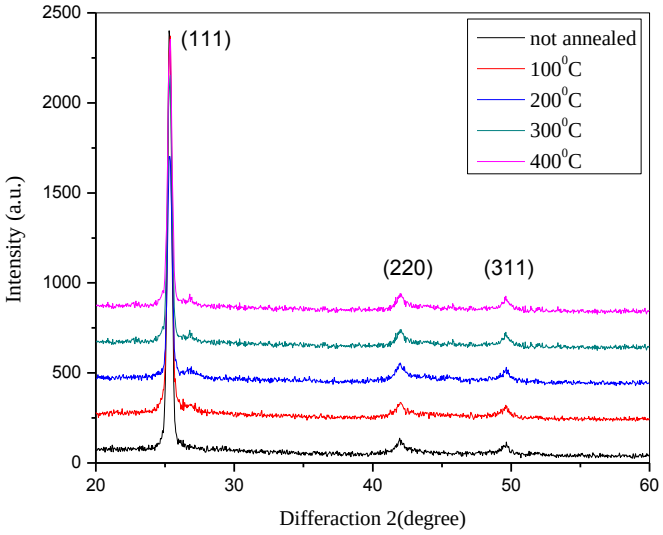

Fig. 1. X-ray pattern of Cu doped and annealed ZnTe thin films

The lattice parameter *'a'* for (hkl) values has been calculated by using the following expression [13],

$$d = \frac{a}{\sqrt{h^2+k^2+l^2}} \quad (1)$$

The grain/crystallite size *'D'* of these Cu doped ZnTe thin films was calculated from XRD patterns using Debye-Scherrer's formula [14].

$$D = \frac{0.9\lambda}{\beta cos\theta} \quad (2)$$

Where *'λ'* is the wavelength of radiation used, *'β'* the full width half maximum, and *'θ'* is the diffraction angle. Fig 2 show the crystallite size variations of sample as doped and samples annealed ZnTe thin films.

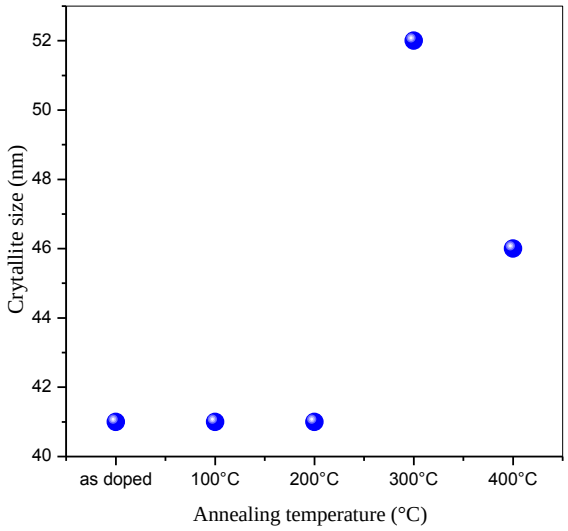

Fig. 2. Crystallite size variations of sample as doped and samples annealed ZnTe thin films

The micro strain *'ε'* of these films was estimated using following formula [15].

$$\varepsilon = \frac{\beta cos\theta}{4} \tag{3}$$

The dislocation density *'δ'* of these thin films was estimated using the following equation [16].

$$\delta = \frac{1}{D^2} \tag{4}$$

Where *'D'* is the grain/crystallite size calculated from equation '1'. These calculated structural parameters are given in table 3. The crystallite size remained unaffected up to annealing temperature of 200°C, which showed that Cu was not diffused properly for these annealing temperatures. When thin films were annealed further then crystallite size became larger for 300°C that showed settlement of dopant atoms. Crystallite size became smaller for further annealing temperature at 400°C.

Table 3: Calculated structural parameters of doped and annealed ZnTe thin films

Sample	Lattice constant (Å)	Crystallite size (nm)	Microstrain (x10^{-4})	Dislocation density x10^{12} (lines/m^2)
Not annealed	6.0924	41	8.374	5.836
100°C	6.0863	41	8.374	5.836
200°C	6.0940	41	8.374	5.837
300°C	6.0938	52	6.700	3.736
400°C	6.0801	46	7.535	4.725

Raman spectra of Cu doped ZnTe thin films are shown in Fig 3. Three pronounced peaks are located at Raman frequencies 207, 410 and 614 cm^{-1}, which are well matched with the literature [17-19].

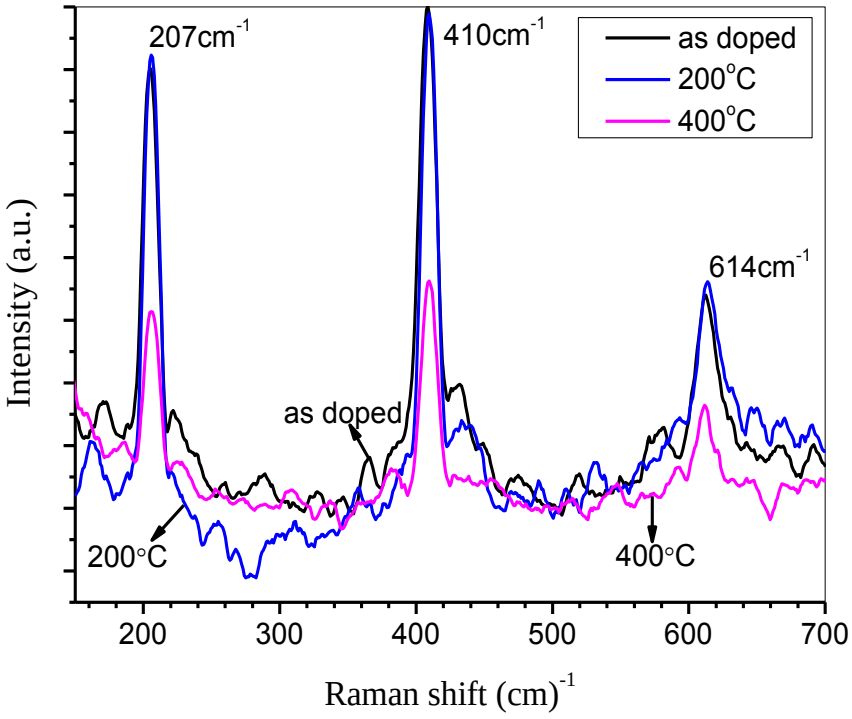

Fig. 3. Raman spectra of Cu doped ZnTe thin films; as doped sample and after annealing

4.2 Optical characterization

The optical transmission spectra of Cu doped and annealed at different temperatures ZnTe thin films are shown in Fig 4. Small shift in absorption edges of samples was observed. These optical transmission spectra have also been used to determine the band gap energies of these thin films. Transmission% of these samples found annealing temperature dependent which became lower for annealing up to 300°C. The absorption coefficient 'α' was calculated from the following relation.

$$\alpha = -\frac{lnT}{t} \tag{5}$$

Where 'T' is transmission and 't' is the thickness of thin films.

The relationship between the absorption coefficient 'α' and the incident photon energy '$h\nu$' is governed by the following relation [20].

$$\alpha h\nu = B\left(h\nu - E_g\right)^n \tag{6}$$

where, 'h' is Planck's constant, 'ν' is the frequency of the radiation, 'n' is a constant which depends on the nature of transition and 'n' is a number (n =1/2, 3/2 or 2), depending on whether the transition is direct-allowed, direct-forbidden, indirect-allowed or indirect forbidden. In the present study the plots of $(\alpha h\nu)^2$ vs $h\nu$ showed a linear portion as given in the Fig 5. This indicated that the relation given in equation '6' holds good for these doped and annealed ZnTe thin films if '$n = {}^1/_2$'. This indicated that optical transition for these thin films is direct transition. Then the relation given in the equation '6' became,

$$(\alpha h\nu)^2 = B\left(h\nu - E_g\right) \tag{7}$$

In the relation given in the equation '7' the absorption coefficient, 'α' is related to the optical band gap 'E_g'by extrapolating the linear portions of the curves and x-intercept for zero absorption coefficients gave the optical band gap values and are shown in Fig 5. The band gap values were varied from 2.22 to 2.19 eV for different annealing temperatures. It could be hypothesize that Cu doping introduced extra energy levels close to the valance band of ZnTe thin films which reduced the band gap energy, same behavior of Cu doping for band gap in ZnTe thin films was also observed by other researchers [21].

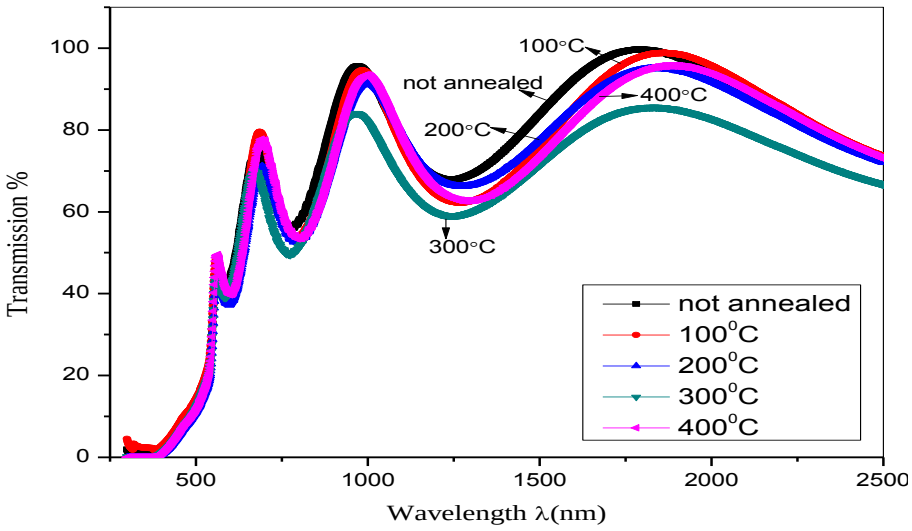

Fig. 4. Transmission spectra of Cu doped and annealed ZnTe thin films

Optical density (OD) which is the measure of transmittance of an optical medium for a given wavelength was calculated from transmission data given in equation '8' [22] and is shown in Fig 6,

$$OD = Log_{10}\frac{1}{T} \tag{8}$$

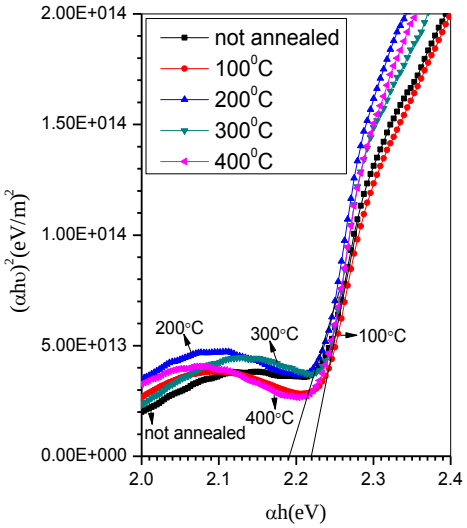

Fig. 5. Plots of $(\alpha h\nu)^2$ vs hν of Cu doped and annealed ZnTe thin films

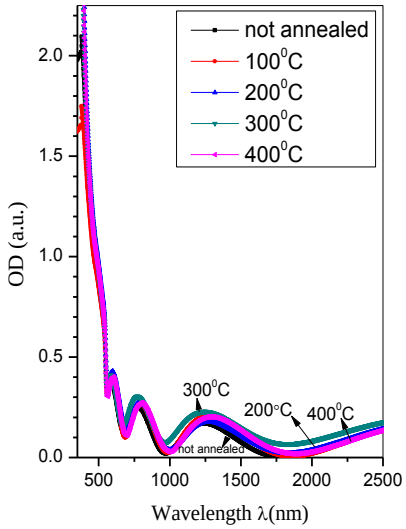

Fig. 6. Optical density(OD) vs wavelength of Cu doped and annealed ZnTe thin films

4.3 Conductivity type determination

The conductivity type of Cu doped ZnTe films was investigated by hot probe method measuring the potential difference between a hot and cold contact. For comparison and reference, we used n-type Si substrate/wafer. Keeping one probe hot compared to the other, thermal gradient generated current in the wafer and the electron current in n-type Si wafer produced a potential [23]. If samples have the same direction of potential, conductivity will be n-type and the corresponding reasoning leads to the opposite potential for p-type conductivity. All Cu doped ZnTe thin films were found to be p-type.

4.4 *I-V* measurements

In order to perform current-voltage (*I-V*) characteristics and conductivity type measurements, the coplanar circular Molybdenum (Mo) metal contacts were deposited on the front face of the films surfaces by DC magnetron sputtering at the chamber ambient temperature. Area of each deposited circular contact was 3.14 mm^2 and separation between two adjacent contacts was 3mm. Typical (*I-V*) characteristics were determined by two-probe technique using tungsten probes. Keithley 4200 semiconductor characterization system was used for the measurements. A box sample holder was used to enable measurements in the dark. These *I-V* characteristics were recorded at the room temperature. For all Cu doped ZnTe samples these measurements showed linear behavior and lines pass through the origin for both negative and positive characteristics as shown in Fig 7. This observation showed ohmic nature of the Cu doped ZnTe samples for the current and the applied voltage. The resistivity of as doped sample was 148 Ω-cm, after annealing it was decreased and reduced to 35 Ω-cm for a sample annealed at 400°C, which is better compared Cu doped ZnTe thin films prepared by close space sublimation [24]. Obtained values of resistivity are given in the table 4. Dependency of resistivity on annealing temperature is given in Fig 8.

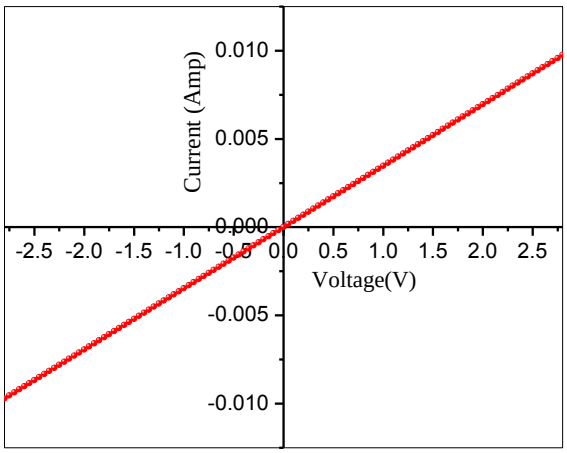

Fig. 7. I-V characteristics of a typical Cu doped ZnTe thin film.

Table 4: Resistivity of Cu doped ZnTe thin films annealed at different temperatures

Annealing temperature (^{o}C)	Resistivity (Ω-cm)
Not annealed	148
100	141
200	55
300	35
400	30

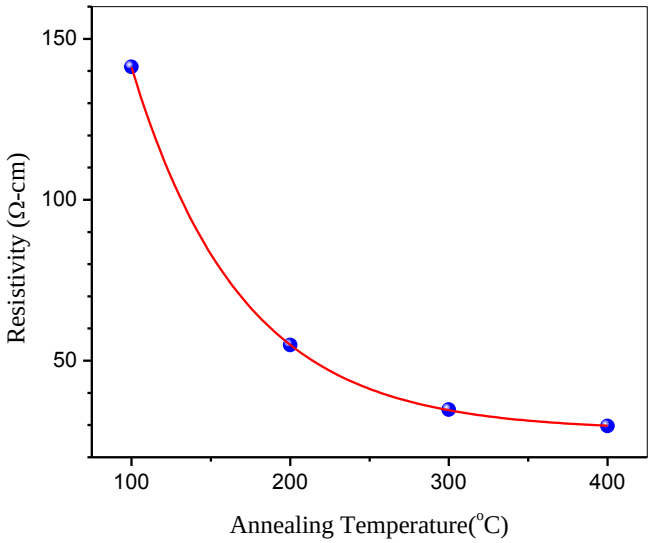

Fig. 8. Dependency of resistivity on annealing temperature of Cu doped ZnTe thin films

5. Conclusions

ZnTe thin films were prepared on glass substrates by thermal evaporation and were successfully doped by Cu with ion exchange technique. All samples were immersed for same time (20 minutes) in Cu $(NO_3)_2$ solution (1g/1000ml) and nearly same amount of Cu (~12 at.%) was found for all doped films. Annealing at different temperatures after doping affected the physical properties of thin films. Optical band gap decreased with annealing upto 300°C, which confirmed the incorporation of the Cu atoms in the ZnTe thin films. The resistivity of un-annealed sample was 148 Ω-cm and after annealing at 400°C it was reduced to 30 Ω-cm. The conductivity type of all Cu doped ZnTe thin films was found to be p-type. These findings can help in the CdTe TFSCs device fabrication.

Acknowledgement

This work was supported by Higher Education Commission Pakistan through "Indigenous 5000 Scholarship Program" HEC is gratefully acknowledged for this support. The authors would like to thank Dr. Arshad Saleem Bhatti, Dr. Nazar Abbas Shah, and Manzar Abbas for providing some of the experimental facilities and for their valuable discussions about this work. One of the authors (G.H. Tariq) is also grateful to the Department of Education, Govt. of the Punjab, Pakistan for granting a study leave for this work.

References

[1] B. A. Korevaar, A. Halverson, J. Cao, J. Choi, C. Collazo-Davila, W. Huber, Thin Solid Films **535**, 229 (2013).
[2] A. Salavei, I. Rimmaudo, F. Piccinelli, A. Romeo, Thin Solid Films **535**, 257 (2013).
[3] V. Krishnakumar, A. Barati, H. J. Schimper, A. Klein, W. Jaegermann, Thin Solid Films **535**, 233 (2013).
[4] M. Hädrich , C. Heisler, U. Reislöhner, C. Kraft, H. Metzner, Thin Solid Films **519**, 7156 (2011).
[5] C. Narayanswamy, T. A. Gessert, S. E. Asher, Presented at the National Center for Photovoltaics Program Review Meeting Denver, Colorado September 8-11, (1998).
[6] D. Rioux, D. W. Niles, H. Höchst, J. Appl. Phys. **73**, 8381(1993).
[7] B. Spath, J. Fritsche, F. Sauberlich, A. Klein, W. Jaegermann, Thin Solid Films **480**, 204 (2005).
[8] A. K. S. Aqili, A. J. Saleh, Z. Ali, S. Al-Omari, J. Alloy Compd. **520**, 83 (2012).
[9] J. Pattar, S. N. Sawant, M. Nagaraja, N. Shashank, K. M. Balakrishna, G. Sanjeev, H. M. Mahesh, Int. J. Electrochem. Sci. **4**, 369 (2009).
[10] G. H. Tariq, K. Hutchings, D.W. Lane, K. D. Rogers, M. Anis-ur-Rehman, J. Phys. D: Appl. Phys. **46**, 485302 (2013).
[11] T. A. Abbas, J.M. Ahmad, J. Electron. Device. **17**, 1413 (2013).
[12] M. B. Rabeh, R. Touatti, M. Kanzari, International Journal of Engineering Practical Research (IJEPR) **2**, 71 (2013).
[13] S. R. Vishwakarma, A. Kumar, S. Das, A. K. Verma, R.S.N. Tripathi, Chalcogenide Letters **10**, 239 (2013).
[14] B. D. Cullity, S. R. Stock, Elements of X-Ray Diffraction 3rd ed., Prentice Hall, New York (2001).
[15] Z. R. Khan, M. Zulfequar, M. S. Khan, Mater. Sci. Eng. B **174**, 145 (2010).
[16] S. Lalitha, R. Sathyamoorthy, S. Senthilarasu, A. Subbarayan, K. Natarajan, Sol. Energy Mater. Sol. Cells **82**, 187 (2004).
[17] K. Ersching, C. E. M. Campos, J. C. de Lima, T. A. Grandi, S. M. Souza, D. L. da Silva, P. S. Pizani, J. Appl. Phys. **105,** 123532 (2009).

[18] V. S. Vinogradov, G. Karczewski, I. V. Kucherenko, N. N. Melnik, and P. Fernandez, Phys. Solid State, **1,** 164-167(2008).
[19] C. S. Yoon, and S. J. Nam, New Physics: Sae Mulli **64**, 512-517 (2014).
[20] L. A. Wahab, H. A. Zayed, A. A. Abd El-Galil, Thin Solid Films **520**, 5195 (2012).
[21] V. S. John, T. Mahalingam, J. P. Chu, Solid State Electron. **49**, 3 (2005).
[22] W. Mahmood, N. A. Shah, S. Akram, U. Mehboob, U. S. Malik, M. U. Sharaf, Chalcogenide Letters **10**, 273 (2013).
[23] S. M. Sze, Physics of Semiconductor Devices 2nd ed., Wiley & Sons, New York (1981).
[24] W. Mahmood, and N. A. Shah, Curr. Appl. Phys. **14,** 282-286 (2014).